High-Rate Space–Time Layered OFDM

Yan Xin, *Student Member, IEEE,* and Georgios B. Giannakis, *Fellow, IEEE*

***Abstract*—We derive a layered space–time scheme for multi-antenna orthogonal frequency-division multiplexed transmissions over frequency-selective channels. Compared with existing alternatives, the proposed scheme can attain very high spectral efficiency as well as improved performance. Enhanced diversity gains document its superior performance that is also tested by simulation.**

***Index Terms*—BLAST, frequency-selective channels, linear precoding, multi-antenna systems, OFDM, space–time coding.**

I. Introduction

EPLOYMENT of multiple transmit-and-receive-antennas has triggered excitement in basic and applied research, because multi-antenna communications offer the potential to improve performance and capacity of flat-selective [5], as well as frequency-selective fading channels [2]. When combined with orthogonal frequency division multiplexing (OFDM), multi-antenna transmissions over intersymbol interference (ISI) channels can also afford low-complexity equalization and decoding. Specific multi-antenna systems with OFDM include the Vertical Bell-labs Layered Space–Time (VBLAST) OFDM [7], and the space–time coded (STC) OFDM with ST trellis or block codes [1], [6], [3]. VBLAST-OFDM is "rate-oriented" as it offers high spectral efficiency at an affordable receiver complexity, while STC-OFDM is "performance-oriented" since it is designed to maximize diversity and coding gains. However, the "jack of both trades" is not available: STC-OFDM incurs rate loss that increases with the number of transmit-antennas, while VBLAST-OFDM comes with performance loss because it neither capitalizes fully on transmit-diversity nor it exploits the multipath-diversity that becomes available with ISI channels.

It is the objective of this letter to bridge this gap, and develop a high-rate layered OFDM scheme with high-performance, and flexibility to enable desirable tradeoffs among rate, performance, and receiver complexity. We reach these goals for *frequency-selective* channels by wedding the OFDM subcarrier grouping ideas we put forth in [6], with linear constellation precoding (LCP) tools [4], [8], and the diagonal (D)BLAST architecture that was originally proposed for *flat-fading* channels in [5].

Manuscript received January 9, 2002. The associate editor coordinating the review of this letter and approving it for publication was Prof. R. S. Blum. This work was supported by the National Science Foundation under NSF Wireless Initiative Grant 9979442, and by the ARL/CTA under Grant DAAD19-01-2-011. This paper appeared in part in the *Proceedings of the Conference on Information Sciences and Systems*, Princeton, NJ, March 2002.

The authors are with the Department of Electrical and Computer Engineering, University of Minnesota, Minneapolis, MN 55455 USA (e-mail: yxin@ ece.umn.edu; georgios@ece.umn.edu).

Publisher Item Identifier S 1089-7798(02)05089-5.

Notation: Bold lower (upper) case fonts will be used to denote column vectors (matrices); $(\cdot)^T$, $(\cdot)^{\mathcal{H}}$, and $[\cdot]_{ij}$ will represent transpose, Hermitian, and the (i, j)th entry of a matrix, respectively.

II. Precoding, DBLAST, and OFDM

Consider a multi-antenna system with N_t transmit- and N_r receive-antennas, where OFDM transmissions with N_c carriers are employed as depicted in Fig. 1. The fading channel between the mth transmit- and the nth receive-antenna is frequency-selective with discrete-time baseband equivalent finite-impulse response (FIR) coefficients collected in the $(L+1) \times 1$ vector $\mathbf{h}_{nm} \triangleq [h_{nm}(0), \ldots, h_{nm}(L)]^T$, with $m \in [1, N_t]$, and $n \in [1, N_r]$. We assume that: $(\mathbf{as})$ *the channel vector* $\mathbf{h} \triangleq [\mathbf{h}_{11}^T, \ldots, \mathbf{h}_{1N_t}^T, \ldots, \mathbf{h}_{N_r1}^T, \ldots, \mathbf{h}_{N_rN_t}^T]^T$ *is zero-mean, complex Gaussian, with correlation matrix* $\boldsymbol{R}_h \triangleq E(\mathbf{h}\mathbf{h}^{\mathcal{H}}) > \mathbf{0}$. Notice that we allow even for correlated wireless channels with, e.g., an exponential power delay profile.

The information symbol stream $\{s_i\}$ is first de-multiplexed to N_t substreams, $\{s_{i,m}\}_{m=1}^{N_t}$, one for each transmit-antenna. Every substream, say the mth, is parsed into blocks, each containing N_c symbols, as many as the system carriers. We select $N_c = N_g(L+1)$, and split every block of N_c symbols into N_g groups, each containing $L+1$ symbols. Let $\mathbf{s}_m^{(p)}$ denote the pth $N_c \times 1$ such block of the mth sub-stream. The gth group from this block is denoted by $\mathbf{s}_{g,m}^{(p)}$, and is particularly chosen to contain the $L+1$ symbols $\{s_{lN_g+g,m}^{(p)}\}_{l=0}^{L}$. Forming likewise all N_g groups will turn out to reduce decoding complexity, but as we will see later, when this particular grouping is combined with precoding, it will also enable the maximum diversity gains (see also [6]).

Collecting $\mathbf{s}_{g,m}^{(p)}$ blocks across all N_t antennas, we form the $N_t(L+1) \times 1$ vector $\mathbf{s}_g^{(p)} \triangleq [\mathbf{s}_{g,1}^{(p)T}, \ldots, \mathbf{s}_{g,N_t}^{(p)T}]^T$ on which we apply linear constellation precoding (LCP) to obtain $\boldsymbol{\Theta}\mathbf{s}_g^{(p)}$, where $\boldsymbol{\Theta}$ is the $N_t(L+1) \times N_t(L+1)$ LCP matrix. With reference to Fig. 1, and $\boldsymbol{\theta}_{lN_t+m}^T$ denoting the (lN_t+m)th row of $\boldsymbol{\Theta}$, the (lN_t+m)th entry, $\boldsymbol{\theta}_{lN_t+m}^T\mathbf{s}_g^{(p)}$, of the pth precoded block will form the symbol $l \in [0, L]$ in the gth group of the mth LCP mapper output. Repeating this for all N_g groups of $L+1$ symbols, describes how the N_t input blocks indexed by p (containing N_c symbols each) are mapped via LCP to yield N_t output blocks that are also indexed by p, and each contains N_c symbols. Notice that each output symbol is formed as a linear combination of $N_t(L+1)$ symbols from all N_t input substreams. This is precisely what enables $\boldsymbol{\Theta}$ to collect both transmit- as well as multipath-diversity gains. If instead of $L+1$ symbols, only one symbol is taken per substream as input to the LCP mapper, then $\mathbf{s}_{g,m}^{(p)}$ reduces to a scalar (call it $s_{n_c,m}^{(p)}$ with $n_c \in [1, N_c]$), the LCP matrix (call it $\overline{\boldsymbol{\Theta}}$) becomes $N_t \times N_t$, and

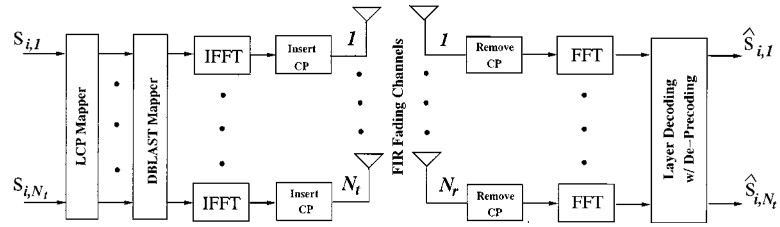

Fig. 1. System model.

each LCP output symbol is now a linear combination of N_t input symbols. Because $\overline{\boldsymbol{\Theta}}$ is smaller than $\boldsymbol{\Theta}$, this leads to reduced complexity de-precoding, but ensures only full transmit-diversity gain.

Consider now a collection of N_l input blocks $\{\mathbf{s}_m^{(p)}\}_{p=1}^{N_l}$ per sub-stream, and the corresponding LCP output blocks, each organized in N_g groups as before: $\{\boldsymbol{\Theta}\mathbf{s}_g^{(p)},\ g \in [1,\ N_g]\}_{p=1}^{N_l}$. With the latter as N_t-branch input, the DBLAST module depicted in Fig. 1 outputs a set of $N_t \times N$ matrices $\{\mathbf{C}_g(l),\ g \in [1,\ N_g],\ l \in [0,\ L]\}$, defined as

$$\mathbf{C}_g(l) \triangleq \begin{bmatrix} c_{g,1}^{(1)}(l) & \cdots & c_{g,1}^{(N_l)}(l) & 0 & \cdots & 0 \\ 0 & c_{g,2}^{(1)}(l) & \cdots & c_{g,2}^{(N_l)}(l) & \ddots & 0 \\ \vdots & \ddots & \ddots & \cdots & \ddots & 0 \\ 0 & \cdots & 0 & c_{g,N_t}^{(1)}(l) & \cdots & c_{g,N_t}^{(N_l)}(l) \end{bmatrix} \tag{1}$$

where the number of columns $N = N_l + N_t - 1$, and $[\mathbf{C}_g(l)]_{mq} \triangleq c_{g,m}^{(p)}(l) \triangleq \boldsymbol{\theta}_{lN_t+m}^T \mathbf{s}_g^{(p)}$, with $p = q - m + 1$, $q \in [m,\ N_l + m - 1]$, and "0" otherwise. Notice that $\mathbf{C}_g(l)$ is structurally reminiscent of the DBLAST code matrix with N_l layers (diagonals) [5]. Since $l \in [0,\ L]$ and $g \in [1,\ N_g]$, we can use $k = lN_g + g$ to index the N_c LCP-mapper output symbols per block, and re-label each entry $[\mathbf{C}_g(l)]_{mq}$ as $[\mathbf{C}(k)]_{mq}$.

We then feed $\mathbf{c}_{mq} \triangleq [[\mathbf{C}(1)]_{mq},\ \ldots,\ [\mathbf{C}(N_c)]_{mq}]^T$ as input to the inverse fast Fourier transform (IFFT) processor of the mth antenna during the qth block (OFDM block-symbol). Next, we take the N_c-point IFFT to obtain $\tilde{\mathbf{c}}_{mq} = \mathrm{IFFT}[\mathbf{c}_{mq}]$, where $[\tilde{\mathbf{c}}_{mq}]_k$ denotes the kth entry of $\tilde{\mathbf{c}}_{mq}$. Prepending the cyclic prefix (CP) of length L, we obtain for each $(m,\ q)$ an $(N_c + L) \times 1$ block $\overline{\mathbf{c}}_{m,q}$ with entries $\{[\tilde{\mathbf{c}}_{mq}]_{N_c-L+1} \cdots [\tilde{\mathbf{c}}_{mq}]_{N_c} [\tilde{\mathbf{c}}_{mq}]_1 \cdots [\tilde{\mathbf{c}}_{mq}]_{N_c}\}$, that we subsequently digital-to-analog convert, pulse shape, and transmit from the mth antenna during the qth block. Our transmitted $N_t \times N(N_c + L)$ space–time code matrix is

$$\overline{\mathbf{C}} \triangleq \begin{bmatrix} \overline{\mathbf{c}}_{1,1}^T & \overline{\mathbf{c}}_{1,2}^T & \cdots & \overline{\mathbf{c}}_{1,N_l}^T & \mathbf{0}^T & \cdots & \mathbf{0}^T \\ \mathbf{0}^T & \overline{\mathbf{c}}_{2,1}^T & \overline{\mathbf{c}}_{2,2}^T & \cdots & \overline{\mathbf{c}}_{2,N_l}^T & \ddots & \vdots \\ \vdots & \ddots & \ddots & \ddots & \cdots & \ddots & \mathbf{0}^T \\ \mathbf{0}^T & \cdots & \mathbf{0}^T & \overline{\mathbf{c}}_{N_t,1}^T & \overline{\mathbf{c}}_{N_t,2}^T & \cdots & \overline{\mathbf{c}}_{N_t,N_l}^T \end{bmatrix}. \tag{2}$$

All the FIR channels are supposed to remain invariant over $N(N_c + L)$ symbol periods. The number of nonzero block entries $\overline{\mathbf{c}}_{mq}^T$ in $\overline{\mathbf{C}}$ is $N_l N_t = (N - N_t + 1)N_t$; and each $1 \times (N_c + L)$ block entry $\overline{\mathbf{c}}_{mq}^T$ carries N_c information symbols (since L redundant symbols correspond to the CP). With these symbols drawn from the alphabet of size $|\mathcal{A}_s|$, our transmission rate is found to be

$$R = \frac{N_t(N - N_t + 1)N_c \log_2 |\mathcal{A}_s|}{N(N_c + L)} \ \text{bps/Hz}.$$

Clearly, selecting $N \gg N_t$ and $N_c \gg L$ leads to very high rates relative to the STC-OFDM in [1], [6], and [3]. To appreciate the flexibility and improved performance of our scheme over the high-rate VBLAST-OFDM in [7], we turn to the receiver and consider the input–output relationship per carrier.

We suppose that carrier synchronization, channel acquisition, timing, and symbol-rate sampling have been accomplished successfully at the receiver. We then remove the CP, and subsequently take the N_c-point FFT of each block at the output of each antenna's receive-filter. Recall that the CP insertion and removal along with the IFFT and FFT taken at the transmitters and receivers, respectively, convert the $N_t N_r$ frequency selective channels to a set of $N_t N_r N_c$ flat fading sub-channels. Specifically, the samples of the qth block at the nth receive-filter output obey the following input–output relationship on the kth carrier:

$$y_{nq}(k) = \sum_{m=1}^{N_t} H_{nm}(k)[\mathbf{C}(k)]_{mq} + w_{nq}(k) \tag{3}$$

where $H_{nm}(k)$ is the frequency response of $\mathbf{h}_{nm}$ at the kth carrier, i.e., $H_{nm}(k) = \sum_{l=0}^{L} h_{nm}(l)e^{-j2\pi lk/N_c}$, and $w_{nq}(k)$s are independent complex Gaussian random variables with zero mean and variance N_0.

Collecting samples $y_{nq}(k)$ from all N_r receive-antennas, and across all N blocks (OFDM block-symbols), for a fixed carrier k, we can recast (3) in a compact matrix form: $\mathbf{Y}(k) = \mathbf{H}(k)\mathbf{C}(k) + \mathbf{W}(k)$, where $[\mathbf{Y}(k)]_{nq} \triangleq y_{nq}(k)$, $[\mathbf{H}(k)]_{nm} \triangleq H_{nm}(k)$, and $[\mathbf{W}(k)]_{nq} \triangleq w_{nq}(k)$. Rewriting k as $k = lN_g + g$, we will pursue decoding per group g, in which the following relationship holds:

$$\mathbf{Y}_g(l) = \mathbf{H}_g(l)\mathbf{C}_g(l) + \mathbf{W}_g(l) \tag{4}$$

where $\mathbf{Y}_g(l) \triangleq \mathbf{Y}(lN_g + g)$, $\mathbf{H}_g(l) \triangleq \mathbf{H}(lN_g + g)$, $\mathbf{C}_g(l) \triangleq \mathbf{C}(lN_g + g)$, and $\mathbf{W}_g(l) \triangleq \mathbf{W}(lN_g + g)$.

In a nutshell, we have developed a layered space time system, which can be viewed as a block version of DBLAST that is combined with OFDM to enable high-rate multi-antenna transmissions over frequency selective channels. As the term DBLAST-OFDM-LCP indicates, our scheme relies also on linear constellation precoding. As we will see next, LCP applied to groups of carriers enriches our high-rate OFDM with multipath diversity at an affordable receiver complexity.

III. Decoding and Performance

Recall from (1) that $[\mathbf{C}_g(l)]_{mq} \triangleq \boldsymbol{\theta}_{lN_t+m}^T \mathbf{s}_g^{(q-m+1)}$. We can see that the information symbols in $\mathbf{s}_g \triangleq [\mathbf{s}_g^{(1)T} \cdots \mathbf{s}_g^{(N_t)T}]^T$ are spread across all the carriers of group g. Thus, we need to consider $\mathbf{C}_g \triangleq [\mathbf{C}_g(0) \cdots \mathbf{C}_g(L)]$ when decoding $\mathbf{s}_g$. Maximum-likelihood (ML) decoding can then be performed per group of carriers to yield: $\hat{\mathbf{s}}_g = \arg\min_{\mathbf{s}_g} \sum_{l=0}^{L} \|\mathbf{Y}_g(l) - \mathbf{H}_g(l)\mathbf{C}_g(l)\|^2$. Albeit computationally heavy, when $\boldsymbol{\Theta}$ is properly designed and $N \geq N_t$, ML decoding enables the maximum possible diversity order $N_t N_r (L+1)$ [9]. This benchmarks the performance of sub-optimum but practical decoders that have lower complexity than ML. Those require $N_r \geq N_t$, and rely on the null-and-cancel decoding [5].

The corresponding algorithm starts with the $N_r \times N_t$ para-unitary matrix $\mathbf{Q}_g(l)$ in the QR factorization of $\mathbf{H}_g(l) = \mathbf{Q}_g(l)\mathbf{U}_g(l)$, and uses $\mathbf{Q}_g(l)$ in (4) to form the matrix $\mathbf{R}_g(l) \triangleq \mathbf{Q}_g^{\mathcal{H}}(l)\mathbf{Y}_g(l) = \mathbf{U}_g(l)\mathbf{C}_g(l) + \mathbf{Q}_g^{\mathcal{H}}(l)\mathbf{W}_g(l)$, where $\mathbf{U}_g(l)$ is an $N_t \times N_t$ upper triangular matrix. Suppose we have decoded the first $(p-1)$ layers that correspond to the first $(p-1)$ diagonals in (1). To decode the block $\mathbf{s}_g^{(p)}$, we consider the $(m,\, p+m-1)$ entry of $\mathbf{R}_g(l)$ that can be written as $\overline{r}_{g,m}^{(p)}(l) = U_{g,m}(l)\boldsymbol{\theta}_{lN_t+m}^T \mathbf{s}_g^{(p)} + \mathcal{L}(\mathbf{s}_g^{(1)}, \ldots, \mathbf{s}_g^{(p-1)}) + v_{g,m}^{(p)}(l)$, where $\mathcal{L}(\mathbf{s}_g^{(1)}, \ldots, \mathbf{s}_g^{(p-1)})$ contains symbols from previously decoded layers, and $v_{g,m}^{(p)}(l)$ denotes the $(m,\, m+p-1)$th entry of $\mathbf{Q}_g^{\mathcal{H}}(l)\mathbf{W}_g(l)$. If all previous layers have been decoded correctly, we can cancel the term $\mathcal{L}(\mathbf{s}_g^{(1)}, \ldots, \mathbf{s}_g^{(p-1)})$ to obtain

$$r_{g,m}^{(p)}(l) = U_{g,m}(l)\boldsymbol{\theta}_{lN_t+m}^T \mathbf{s}_g^{(p)} + v_{g,m}^{(p)}(l). \tag{5}$$

What boosts performance of the nulling-cancelling iteration in our case is the de-precoding step that is needed after the interference nulling to decode $\mathbf{s}_g^{(p)}$ from the LCP blocks $\boldsymbol{\theta}_{lN_t+m}^T \mathbf{s}_g^{(p)}$ in (5). Collecting (5) for $l \in [0, L]$ and $m \in [1, N_t]$, we perform de-precoding per layer p of each group g, based on the block: $\mathbf{r}_g^{(p)} = \mathbf{D}_g^{(p)}\boldsymbol{\Theta}\mathbf{s}_g^{(p)} + \mathbf{v}_g^{(p)}$, where $\mathbf{D}_g^{(p)} \triangleq \mathrm{diag}[U_{g,1}(0) \cdots U_{g,N_t}(0) \cdots U_{g,1}(L) \cdots U_{g,N_t}(L)]$, and $\mathbf{v}_g^{(p)} \triangleq [v_{g,1}^{(p)}(0) \cdots v_{g,N_t}^{(p)}(0) \cdots v_{g,1}^{(p)}(L) \cdots v_{g,N_t}^{(p)}(L)]^T$. This step is implemented using the sphere-decoding (SD) algorithm that is known to exhibit near-ML performance at complexity that is polynomial in the length $N_t(L+1)$ of $\mathbf{s}_g^{(p)}$ [4]. Even lower complexity de-precoding is possible by inverting $\boldsymbol{\Theta}\mathbf{s}_g^{(p)}$ in the zero-forcing or minimum mean-square sense (see [6], [8] for details).

We prove in [9] that under proper conditions on the channel and the precoder, the diversity order with layer decoding (that includes de-precoding) is: $G_d^{(p)} = [N_r N_t - (N_t-1)N_t/2](L+1)$, regardless of the layer $p \in [1, N_l]$. This is in agreement with the original DBLAST scheme applied to flat-fading channels, where the layer decoding order does not affect performance when one assumes that previous layers have been decoded correctly. The $\boldsymbol{\Theta}$s satisfying our conditions in [9] are those we have constructed in [8, eq. (7)].

Fig. 2 depicts the performance comparison between DBLAST-OFDM-LCP and VBLAST-OFDM. Using $N_c = 15$ and $L = 2$, we test two cases for $N_t = N_r = 5$, and $N_t = N_r = 3$ with 16-QAM. We use Reed–Solomon (15, 9) codes for VBLAST-OFDM, and the precoder $\boldsymbol{\Theta}$ of [8, eq. (7)] for DBLAST-OFDM-LCP. Since the transmit-diversity order is high for $N_t = N_r = 5$, we use the sub-optimum precoder $\overline{\boldsymbol{\Theta}}$ to reduce the complexity at the expense of multipath-diversity loss [see discussion before (1)]. To ensure identical transmission rates for VBLAST-OFDM and DBLAST-OFDM-LCP, we choose $N = 5$ when $N_t = N_r = 3$, and $N = 10$, when $N_t = N_r = 5$. The corresponding rates are $R = 6.35$ bps/Hz, and $R = 10.58$ bps/Hz, respectively. Fig. 2 corroborates that DBLAST-OFDM-LCP outperforms VBLAST-OFDM considerably (about 5 dB at $\mathrm{BER} = 10^{-4}$).

In the full version of this work [9], we will study performance with error propagation in the decoding process, and we will also assess the coding gains along with the pertinent complexity-performance-rate tradeoffs even with $N_r < N_t$.

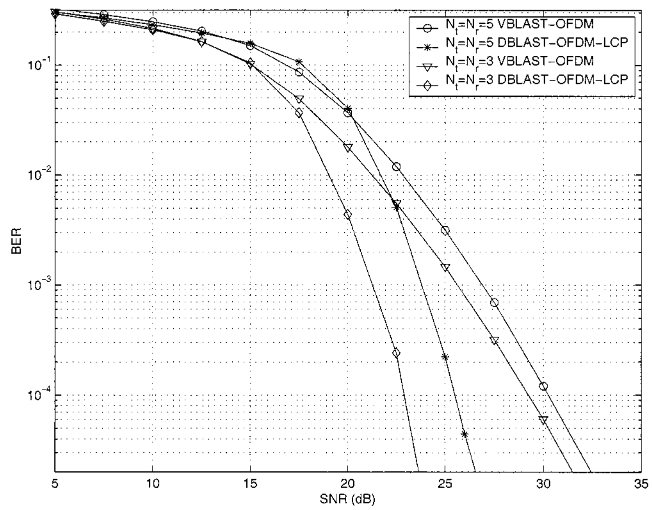

Fig. 2. DBLAST-OFDM-LCP versus VBLAST-OFDM.

References

[1] D. Agrawal, V. Tarokh, A. Naguib, and N. Seshadri, "Space-time coded OFDM for high data-rate communication over wideband channels," in *Proc. IEEE Vehicular Technology Conf.*, Ottawa, ON, Canada, May 1998, pp. 2232–2236.

[2] S. L. Ariyavisitakul, "Turbo space–time processing to improve wireless channel capacity," *IEEE Trans. Commun.*, vol. 48, pp. 1347–1359, Aug. 2000.

[3] R. S. Blum, Y. Li, J. H. Winters, and Q. Yan, "Improved space–time coding for MIMO-OFDM wireless communications," *IEEE Trans. Commun.*, vol. 49, pp. 1873–1878, Nov. 2001.

[4] J. Boutros and E. Viterbo, "Signal space diversity: A power and bandwidth efficient diversity technique for the Rayleigh fading channel," *IEEE Trans. Inform. Theory*, vol. 44, pp. 1453–1467, July 1998.

[5] G. J. Foschini and M. J. Gans, "Layered space–time architecture for wireless communication in a fading environment when using multiple antennas," *Bell Labs. Syst. Tech. J.*, vol. 1, pp. 41–59, 1996.

[6] Z. Liu, Y. Xin, and G. B. Giannakis, "Space–time-frequency coded OFDM over frequency-selective fading channels," *IEEE Trans. Signal Processing*, to be published.

[7] R. J. Piechocki, P. N. Flectcher, A. R. Nix, C. N. Canagarajah, and J. P. McGeehan, "Performance evaluation of BLAST-OFDM enhanced Hiperlan/2 using simulated and measured channel data," *Electron. Lett.*, vol. 37, no. 18, pp. 1137–1139, Aug. 2001.

[8] Y. Xin, Z. Wang, and G. B. Giannakis, "Space–time constellation-rotating codes maximizing diversity and coding gains," in *Proc. GLOBECOM Conf.*, San Antonio, TX, Nov. 25–29, 2001, pp. 455–459.

[9] Y. Xin, G. B. Giannakis, and S. Zhou, "High-rate space–time layered multi-carrier and single-carrier transmissions over frequency-selective channels," *IEEE Trans. Commun.*, in preparation.